



Published in final edited form as:

*J Biomed Nanotechnol.* 2014 May ; 10(5): 856–863.

## ***In Vivo* Imaging of Infection Using a Bacteria-Targeting Optical Nanoprobe**

Ewin N. Tang<sup>1</sup>, Ashwin Nair<sup>1</sup>, David W. Baker<sup>1</sup>, Wenjing Hu<sup>2</sup>, and Jun Zhou<sup>1,\*</sup>

<sup>1</sup>Department of Bioengineering, University of Texas at Arlington, Arlington, TX 76019, USA

<sup>2</sup>Progenitex Inc., 1917 Parktree Drive, Arlington, TX 76001, USA

### **Abstract**

Wound and device-associated infection is a leading cause for morbidity and mortality. As such, rapid and early diagnosis of bacterial colonization is critical to infection treatment. The current diagnostic methods however, are not able to meet this requirement. Therefore, there is a practical need for the development of a new method to rapidly identify colonized bacteria. This study aims to develop optical nanoprobe that can detect and quantify the number of colonized bacteria in real time. To this end, we have synthesized an imaging nanoprobe with three elements: Concanavalin A (Con A) as a bacterial targeting ligand, a nanoparticle carrier, and a near infrared fluorescent dye. An MTS assay revealed that the bacteria nanoprobe is cell compatible. *In vitro* testing further showed that the bacteria nanoprobe had a very high specificity and affinity to bacteria. Using a murine wound and catheter infection model, we found that the bacteria nanoprobe can rapidly detect and quantify the extent of bacterial colonization on wounds and catheters in real time.

### **Keywords**

Bacteria; Wound Infection; In Vivo; Optical Imaging; Nanoprobe; Diagnosis

## **INTRODUCTION**

Trauma, burn, and diabetes patients are most vulnerable to infection, because bacteria can enter through open wounds. It is estimated that > 10 billion dollars are spent in the treatment of these non-healing wounds. Bacteria have often been observed to colonize non-healing wounds and surgical sites, resulting in further tissue damage that prolongs the process of wound healing.<sup>1, 2</sup> In addition, bacterial infection has been linked to the failure of many medical devices, such as prosthetic heart valves, dental implants, joint replacements, renal dialysis/ventricular shunts, intravenous, indwelling urinary and endotracheal catheters.<sup>3–9</sup> Infections contribute greatly to patient care costs, morbidity and even an increased mortality rate. To make the situation worse, there is no rapid and reliable diagnostic technique to detect wound or implant-related infection in clinical practice. Current infection diagnostic methods involve biopsying tissue or implant samples and sending them to a clinical laboratory for bacterial culture, identification of key traits, and related tests.<sup>5</sup> These

\* Author to whom correspondence should be addressed. junzh@uta.edu.

diagnostic methods are labor intensive and time consuming (taking days), costly, and often have low sensitivity. These limitations can substantially delay treatment and drastically increase hospital stay time and treatment costs. These drawbacks necessitate the need for quick and effective ways to diagnose bacterial infection.

Numerous imaging modalities have recently been developed to diagnose different diseases, including trauma, various brain diseases, cancer and inflammation. These include magnetic resonance imaging (MRI), tomography, ultrasound imaging, *Y*-blink imaging, X-ray computed tomography imaging, computed tomography magnetic resonance imaging, and emission tomography imaging.<sup>10–12</sup> However, these methods require the use of specialized equipment and often expensive reagents. On the other hand, optical imaging using fluorescent probes has generated a lot of interest because of its low cost, easy operation, as well as rapid and accurate measurements. Although optical imaging tools have been used to study the pathogenesis of infection, most of the research has focused on tracking luciferase transgenic microorganisms and not detecting pathogenic microorganisms.<sup>13–16</sup> Limited studies have been carried out to identify microorganisms by detecting bacterial cell wall physical and chemical properties, such as the anionic surface of the bacterial cell wall.<sup>17</sup> Unfortunately, the sensitivity of these probes is relatively poor.<sup>17</sup> To overcome these drawbacks, we developed a new low-cost optical imaging probe that can be used non-invasively to detect and quantify the amount of colonized bacteria *in vivo*, reflecting the extent of wound and device-associated infections in real-time.

To this end, an optical imaging probe was designed to have three elements: a bacterial targeting ligand, a polymeric nanoparticle carrier, and a near infrared fluorescent dye. Concanavalin A (Con A) was selected as the bacterial targeting ligand, since it has a high affinity to the  $\alpha$ -D-mannosyl and  $\alpha$ -D-glucosyl-specific groups on the bacterial cell wall.<sup>18, 19</sup> Furthermore, Con A has a relatively low cost and a wide variety of carbohydrate specificities on bacteria cell walls to Gram-positive and Gram-negative bacteria.<sup>20–23</sup> To increase detection sensitivity, Con A was conjugated to the nanoparticle carrier. In addition, for *in vivo* imaging and to avoid overlap with tissue and skin auto-fluorescence, bacteria probes were labeled with a near infrared dye-1,1',3,3,3',3'-Hexamethylindotricarbocyanine iodide (IR750). The ability of bacteria probes to detect and quantify the number of bacteria was tested both *in vitro* and *in vivo*.

## MATERIALS AND METHODS

Bacterial probes were synthesized following published methods.<sup>24</sup> First, amine-functionalized poly (*N*-isopropylacrylamide-*co*-styrene) (PNIPAM-*co*-St) nanoparticles were synthesized via emulsion polymerization.<sup>24</sup> The loading of IR750 dye into the nanoparticles was conducted following previous procedures.<sup>24, 25</sup> Finally, the bacterial nanoprobe was prepared by chemically conjugating Con A onto the IR750-loaded nanoparticles via EDC chemistry.<sup>26</sup> Probe size was determined by Photon Correlation Spectroscopy (ZetaPALS, Brookhaven Instruments Co., Holtsville, NY, USA). The loading efficiency of IR750 dye was estimated as the ratio of the mass of loaded dye, obtained by the calibration curve of IR750, to the mass of dried probes. Absorbance and fluorescence spectra of entrapped IR750 dye were measured by UV-vis spectrophotometer (Lambda 19

Spectrometer, PerkinElmer, MA) and a Tecan Infinite M 200 plate reader (San Jose, CA, USA), respectively. FTIR spectroscopy was performed to confirm effective conjugation of Con A in bacterial probes. To determine Con A conjugation efficiency, FITC-labeled Con A was utilized through conjugation to the nanoparticles at the same conditions as in the preparation of bacterial probes. Using the UV-vis spectrophotometer, conjugation efficiency of Con A was estimated as the ratio of the mass of loaded dye, obtained by the calibration curve of FITC-labeled Con A, to the mass of dried probes.<sup>27</sup> For all studies, control nanoprobe were similarly synthesized without Con A conjugation.

Cytotoxicity evaluation of bacteria optic probes to 3T3 fibroblasts and Raw 264.7 Macrophages was conducted using a standard MTS assay.<sup>24</sup> Briefly, cells were seeded in a 96-well plate at the density of  $1 \times 10^4$  cells/well in DMEM medium supplemented with 10% fetal bovine serum (FBS) + 1% antibiotics for 24 hours with 5% CO<sub>2</sub> at 37 °C. The culture medium in each well was replaced with 200 µL of complete DMEM medium in the presence of various concentrations of probes (0–0.05 mg/ml) and incubated for 24 hours. The medium was removed and cells washed three times with phosphate buffered saline (PBS, pH 7.4). 20 µl of CellTiter 96<sup>®</sup> AQueous One Solution Reagent (Promega, USA) and 100 µl of DMEM medium was added into each well and incubated for 4 hours. The absorbance of the MTS reaction was measured at 490 nm using a SpectraMax 340 Spectrophotometric plate Reader (Molecular Devices, USA).

To assess the ability of the bacteria optical probe to detect live bacteria *in vitro*, Gram-positive *Xen 29 Staphylococcus aureus* was used as a model microorganism. *Staphylococcus aureus* ( $1.6 \times 10^8$  CFU/ml) were incubated with different concentrations of the bacteria nanoprobe or control nanoprobe for 30 minutes and followed with 3× washes of sterile PBS. The fluorescence intensities of nanoprobe were then determined using the fluorescent plate reader (excitation: 760 nm; emission: 830 nm).

To determine whether the bacteria nanoprobe can quantify the number of bacteria, either the bacteria nanoprobe or the control nanoprobe (200 µg/ml) was incubated with different concentrations of bacteria ( $1.6 \times 10^8$ ,  $0.8 \times 10^8$ ,  $0.4 \times 10^8$ ,  $0.2 \times 10^8$ ,  $0.1 \times 10^8$  and  $0.05 \times 10^8$  colony forming units/ml) for 30 minutes at 37 °C. The bacteria were washed with sterile PBS three times to remove unbound probe and the fluorescence intensities were measured using a Kodak *In-Vivo* FX Pro system (*f*-stop: 2.5, excitation filter:  $760 \pm 30$  nm, emission filter:  $830 \pm 30$  nm,  $4 \times 4$  binning; Carestream Health, Rochester, NY, USA).

To confirm the ability of the bacteria nanoprobe to detect infected catheters, polyurethane (PU) catheters from Sentry Medical Products (Green Bay, WI) were incubated with bacteria ( $1.6 \times 10^9$  colony forming units/ml) for 4 hrs followed by 3× wash with PBS buffer. The bacteria-colonized catheters were then incubated with the bacteria nanoprobe or the control nanoprobe (20 µg/ml) for 4 minutes. After washing off unbound nanoprobe, *in vivo* imaging was taken in a Kodak *In-Vivo* FX Pro system (*f*-stop: 2.5, excitation filter:  $760 \pm 30$  nm, emission filter:  $830 \pm 30$  nm,  $4 \times 4$  binning). To detect infected wound and catheters *in vivo*, Balb/C mice (female, 20–25 g/mouse; Taconic Farms, Germantown, NY) were used and cared for in accordance with the guidelines laid by the Institutional Animal Care and Use Committee at the University of Texas at Arlington. To create infected wounds, three 0.5-

cm horizontal dorsal incisions were made through the skin and panniculus carnosus muscle of Balb/C mice following sedation. The wound was left uncovered. Some of the wounds were inoculated with  $\sim 2 \times 10^6$ – $5 \times 10^7$  luciferase transgene *Staphylococcus aureus* Xen 29 strain/50  $\mu$ l as described earlier.<sup>28</sup> To simulate catheter-associated infection, PU catheters measuring 1 cm in length were implanted on either side on the dorsal subcutaneous space of mice such that 0.4 cm extended out of the incision site. An hour later, 20  $\mu$ l of saline was dropped onto the incision site of the control catheters while the same volume of luciferase transgene *Staphylococcus aureus* ( $3.2 \times 10^7$  colony forming units/20  $\mu$ l/catheter) was dropped on the incision site and outer surfaces of the catheter. At various time points (24, 48 and 72 hours) following bacterial inoculation, 20  $\mu$ l of bacteria probes (4  $\mu$ g/wound) was dropped onto the incision sites. After incubation for 5 minutes, the site was washed three times with sterile PBS and the *in vivo* fluorescence images were recorded following background subtraction. Data analysis was performed using Carestream Molecular Imaging Software, Network edition 4.5 (Carestream Health, Rochester, NY, USA).

All the data were expressed as mean  $\pm$  Standard error of the mean (SEM). To compare the difference between groups, one-way analysis of variance (ANOVA) and student *t*-test were conducted. A value of  $p < 0.05$  was considered to be significant. Correlations were determined by regression analysis and the coefficient of determination ( $R^2$ ).

## RESULTS

An *in vivo* imaging approach was explored for rapid and accurate diagnosis of wound or catheter-related infections. The concept of detecting bacteria colonized on a wound is illustrated in Figure 1(A). The probes were fabricated using PNIPAM-*co*-St nanoparticles. The probe size was found to be  $204 \pm 4$  nm using Photon Correlation Spectroscopy (Fig. 1(B)). A polydispersity of 0.137 indicates good monodispersity, while the measurement of optical properties reveals that the probe has two distinct peaks with absorbance and emission of  $\sim 758$  nm and  $\sim 792$  nm, respectively (Fig. 1(C)). As reported in our previous publication, the hydrophobic polystyrene domains entrapping IR750 dye are able to isolate the dye from oxidative agents, such as dissolved oxygen, and thus prolong the photostability of the nanoprobe.<sup>24</sup> The IR750 dye loading efficiency was estimated to be 3.1% (w/w) based on a standard curve between dye concentration and UV absorbance with the equation  $y = 14.408x - 0.0303$  ( $R^2 = 0.99$ ). Since coupling of the carboxylic groups of Con A with amine groups of the nanoparticles leads to the formation of amide bonds, the bands of amide groups were measured using FTIR to support the conjugation of Con-A with the nanoparticle. As expected, from the FTIR spectra (Fig. 1(D)), enlarged bands of amide I ( $1630 \text{ cm}^{-1}$ ) and amide II ( $1520 \text{ cm}^{-1}$ ) were found in Con A-conjugated nanoprobe, indicating successful conjugation of Con A to the probe.<sup>18</sup> By dividing the amount of Con A over the weight of the nanoprobe, it is estimated that 6 nanomoles of Con A were bound per milligram of the probe.

To determine the cytotoxicity of bacteria probes, we carried out experiments using 3T3 fibroblasts, Raw 264.7 macrophages (*MΦ*s), and an MTS assay (Figs. 2(A)–(B)). The cells were incubated with different concentrations of the bacteria probes for 24 hours. The number of live cells was determined and then compared with the untreated control to

calculate the percentage of cell survival. We found that bacteria probes triggered no statistically significant cytotoxicity up to 0.0025 mg/ml (Fig. 2(A)). In the case of 3T3 fibroblasts, approximately 10–20% cell toxicity was found at bacteria probe concentrations between 0.01 and 0.05 mg/ml. On the other hand, for Raw 264.7 macrophages (MΦs), nanoprobe have very low or no apparent cytotoxicity up to 0.05 mg/ml (Fig. 2(B)). To determine the affinity of the probe to bacteria, *Staphylococcus aureus*, a persistent microbe responsible for wound or catheter-related infections, was chosen.<sup>29, 30</sup> *Staphylococcus aureus* ( $1.6 \times 10^8$ /ml) was incubated with different concentrations of the bacteria probe and the control nanoprobe for 30 minutes followed by 3× wash with sterilized PBS. The bacteria-associated fluorescent signals were then measured using a fluorescent plate reader. We found that the bacteria probe has a high affinity to the bacteria. However, the control probe had little to no affinity to bacteria (Fig. 2(C)). In addition, there was a good relationship between the probe concentrations and fluorescent intensity (Fig. 2(C)). These results suggest that the probes used in this work did not saturate the binding sites on the bacterial wall.

Bacterial infection is often associated with the colonization of a large number of microorganisms. To assess the extent of bacterial infection, it is essential to quantify the amount of colonized bacteria. For that, we evaluated whether the bacteria probes can be used to measure the amount of live bacteria. Different amounts of *Staphylococcus aureus* were incubated with bacteria probes or control probes (100 µg/ml) for 30 minutes prior to being washed 3× with sterilized PBS. Some of the samples were placed on top of glass slides and then air-dried in a dark chamber. Indeed, fluorescence intensity is strongly dependent on bacterial concentration. Strong fluorescent signals were emitted from the highest concentrations of bacteria ( $1.6 \times 10^8$ /ml) while weak fluorescent intensities were found with lower bacteria concentrations (Fig. 3(A)). There was a linear relationship between bacteria numbers and associated fluorescence intensities ( $R^2 = 0.947$ ) (Fig. 3(B)).

Next, we explored the possibility of using bacteria probes to detect catheter-associated infection *in vitro*. Catheters were incubated with bacteria-contaminated saline for 4 hours and then incubated with either the bacteria probe or control probe for 4 minutes prior to PBS washing. The presence of the bacteria on the catheters was quantified to reveal an almost 7× increase in fluorescence due to probe binding on infected catheters in comparison to the control probe and sterile catheters (Fig. 4). This suggests that bacteria determination is very specific, as the control probe-treated catheters show no fluorescence. The overall observations support the idea that the newly-fabricated bacteria probe can be used to detect bacteria colonization on catheters *in vitro*.

The next challenge was to determine whether the bacteria nanoprobe can be used to detect wound infection *in vivo*. For this investigation, the wound site was inoculated with different numbers of *Staphylococcus aureus*. The wounds were then immersed with bacterial probes (40 µg/ml) for 10 minutes, washed with sterile saline, and then imaged. As expected, an increasing number of bacteria (represented by luminescent intensities) were associated with a rising intensity of bacteria probe fluorescence (Fig. 5(A)). In addition, there is a very high correlation ( $R^2 = 0.9283$ ) between bacterial transgene luminescent intensities and bacterial probes' fluorescence intensities (Fig. 5(B)). To explore the possibility of using bacterial

probes to detect infected catheters, we established a mouse model with transcutaneous implantation of bacteria-infected and sterile catheters. After implantation for different periods of time (1, 2, and 3 days), bacteria nanoprobe were dropped onto the catheter sites, washed with sterile saline, and then imaged. By day 1 following implantation, we found a much greater (2×) localization of the probes at the infected site as opposed to the control which had no infection (Fig. 5(C)). Interestingly, this trend was also observed on day 2 with almost 4× more accumulation of bacteria probes surrounding the infected catheters. By day 3, the fluorescence from the probes increased by almost 5× as compared to control. It should also be noted that during this period the number of bacteria was also observed to increase by 2×. Quantitative analysis of the fluorescence intensities corroborates this observation (Fig. 5(D)).

## DISCUSSION

Development of nanotechnology and NIR probes has significantly helped advance our understanding of various biological processes. A booming ageing population and tremendous increase in the demand for medical devices and prosthetics also brings forth concerns of wound and device-centered infection and other serious pathological conditions. In particular, full blown Staphylococcal infections related to catheter implants and prosthetics are very difficult to eradicate, and hence it is crucial that they be detected at a very early stage. Improper and delayed diagnosis of such infections can often have dire consequences. There is an emerging need to develop a strategy to quickly and non-invasively detect bacterial colonization in real time.

In this study, a nano-sized optical and bacteria-targeting probe was fabricated. This nanoprobe was loaded with a NIR dye to take advantage of NIR-based fluorescence optical imaging. In addition, this probe was labeled with Con A, a low cost lectin-binding protein that has been shown to interact with surface mannose residues of microorganisms like *S aureus* as well as *E coli*.<sup>31, 32</sup> It has a wide variety of carbohydrate specificities to the polysaccharides on the cell walls of both Gram positive and Gram negative bacteria.<sup>20–23</sup> Additionally, Con A has a high affinity to the  $\alpha$ -D-mannosyl and  $\alpha$ -D-glucosyl groups on most Gram-positive bacteria walls.<sup>18</sup> It should be noted that a number of other compounds similarly possess a high affinity to the bacterial wall. For example, eosinophil cationic protein has been shown to have a high affinity to both Gram positive and Gram negative strains of bacteria.<sup>33</sup> In addition, cell membrane affinity chromatography has been recently developed to identify novel peptides for different microorganisms.<sup>34</sup> Such compounds can be easily incorporated into our probe to explore further applications in the future. It must also be noted that fluorescent probes such as dihydroethidium, dihydrorhodamine, and sulphonate ester-based dyes have been used for detecting various biological processes, but are plagued by photobleaching, high toxicity, and low emission wavelengths.<sup>35, 36</sup> The overall results from this study surpass these shortcomings and indicate a high conjugation efficiency of the targeting ligand Con A to the bacteria probe.

Particles often interact with cells via phagocytosis—cellular uptake of the particles. To reduce probe uptake by the cells and potential adverse immune responses from the body, bacteria probes were fabricated with PNIPAM-*co*-St particles having a uniform diameter of



~200 nm. Additionally, the hydrophobic properties of polystyrenes reduces the chance of chromophore photobleaching by moisture, therefore, photostability of the physically-entrapped chromophore can be substantially enhanced.<sup>24</sup> On the other hand, since the amphiphilic molecular structure of PNIPAM nanoparticles can lead to the formation of a strong interfacial hydration layer, PNIPAM-based particles usually have little/no cytotoxic effect on tissues or cells.<sup>37, 38</sup> Without exception, the bacteria nanoprobe in this study were found to lack cytotoxicity to fibroblasts as well as macrophages. In addition, they were highly specific to bacteria. Our results demonstrate the specificity of the bacteria nanoprobe and its ability to quantify bacterial numbers *in vitro*. Furthermore, using wound and catheter-related infection models, our studies show that the bacteria nanoprobe are able to detect and quantify an increased presence of bacteria. This is a positive indication of the nanoprobe's various potential for *in vivo* applications.

We believe that this research will provide a new method not just to visualize the presence of microorganisms but also provide quantitative measurement and distribution of these invaders. These newly developed bacteria nanoprobe can greatly improve our understanding of the processes and factors governing infection. Furthermore, this optical imaging technique may have practical applications in the evaluation and diagnosis of various infection related complications in the clinic without sophisticated laboratory facilities and a prolonged processing time.

In summary, a Con A-conjugated IR750-loaded nanoparticle has been developed as an optical nanoprobe to detect and quantify the extent of bacteria colonization and associated infection. *In vitro* studies demonstrate that the nanoprobe has a high affinity and sensitivity to bacteria. Using a mouse model of bacteria-colonized wound and catheter implants, we found that the bacteria nanoprobe can measure the extent of wound bacterial colonization and catheter-associated infection *in vivo*.

## Acknowledgments

This work was supported by a NIH grant R43 AR064650. The authors acknowledge Ms. Jada Wang for her assistance during the beginning of this work.

## REFERENCES

1. Edwards R, Harding KG. Bacteria and wound healing. *Curr. Opin. Infect. Dis.* 2004; 17:91. [PubMed: 15021046]
2. Bode LG, Kluytmans JA, Wertheim HF, Bogaers D, Vandenbroucke-Grauls CM, Roosendaal R, Troelstra A, Box AT, Voss A, van der Tweel I, van Belkum A, Verbrugh HA, Vos MC. Preventing surgical-site infections in nasal carriers of *Staphylococcus aureus*. *N. Engl. J. Med.* 2010; 362:9. [PubMed: 20054045]
3. Pye AD, Lockhart DE, Dawson MP, Murray CA, Smith AJ. A review of dental implants and infection. *J. Hosp. Infect.* 2009; 72:104. [PubMed: 19329223]
4. Eggimann P, Sax H, Pittet D. Catheter-related infections. *Microbes Infect.* 2004; 6:1033. [PubMed: 15345236]
5. Raad I, Hanna H, Maki D. Intravascular catheter-related infections: Advances in diagnosis, prevention, and management. *Lancet Infect. Dis.* 2007; 7:645. [PubMed: 17897607]
6. O'Grady NP, Alexander M, Dellinger EP, Gerberding JL, Heard SO, Maki DG, Masur H, McCormick RD, Mermel LA, Pearson ML, Raad II, Randolph A, Weinstein RA. Guidelines for the

prevention of intravascular catheter-related infections, centers for disease control and prevention. *MMWR Recomm. Rep.* 2002; 5:11.

7. O'Grady NP, Alexander M, Burns LA, Dellinger EP, Garland J, Heard SO, Lipsett PA, Masur H, Mermel LA, Pearson ML, Raad II, Randolph AG, Ruup ME, Saint S. Guidelines for the prevention of intravascular catheter-related infections. *Clin. Infect. Dis.* 2011; 52:e162. [PubMed: 21460264]
8. O'Grady NP, Alexander M, Burns LA, Dellinger EP, Garland J, Heard SO, Lipsett PA, Masur H, Mermel LA, Pearson ML, Raad II, Randolph AG, Ruup ME, Saint S. Summary of recommendations: Guidelines for the prevention of intravascular Catheter-related Infections. *Clin. Infect. Dis.* 2011; 52:1087. [PubMed: 21467014]
9. O'Grady NP, Alexander M, Burns LA, Dellinger EP, Garland J, Heard SO, Lipsett PA, Masur H, Mermel LA, Pearson ML, Raad II, Randolph AG, Ruup ME, Saint S. Guidelines for the prevention of intravascular catheter-related infections. *Am. J. Infect. Control.* 2011; 39:S1. [PubMed: 21511081]
10. Jin M, Hao G, Sun X, Chen W. Nanoparticle-based positron emission tomography and single photon emission computed tomography imaging of cancer. *Rev. Nanosci. Nanotechnol.* 2012; 1:3.
11. Wolf, GL. Handbook of Targeted Delivery of Imaging Agents. Torchilin, VP., editor. Boca Raton, FL: CRC Press; 1995. p. 3-22.
12. Zhou J, Hao G, Weng H, Tsai Y, Sun X, Tang L. *In vivo* evaluation of medical device-associated inflammation using a macrophage-specific positron emission tomography (PET) imaging probe. *Bioorg. Med. Chem. Lett.* 2013; 23:2044. [PubMed: 23481649]
13. Doyle TC, Burns SM, Contag CH. *In vivo* bioluminescence imaging for integrated studies of infection. *Cell Microbiol.* 2004; 6:303. [PubMed: 15009023]
14. Hutchens M, Luker GD. Applications of bioluminescence imaging to the study of infectious diseases. *Cell Microbiol.* 2007; 9:2315. [PubMed: 17587328]
15. Sato A, Klaunberg B, Tolwani R. *In vivo* bioluminescence imaging. *Comp. Med.* 2004; 54:631. [PubMed: 15679260]
16. Sharma PK, Engels E, Van Oeveren W, Ploeg RJ, van Henny der Mei C, Busscher HJ, Van Dam GM, Rakhorst G. Spatiotemporal progression of localized bacterial peritonitis before and after open abdomen lavage monitored by *in vivo* bioluminescent imaging. *Surgery.* 2009; 147:89. [PubMed: 19733882]
17. Leevy WM, Gammon ST, Johnson JR, Lampkins AJ, Jiang H, Marquez M, Piwnica-Worms D, Suckow MA, Smith BD. Noninvasive optical imaging of staphylococcus aureus bacterial infection in living mice using a Bis-dipicolylamine-Zinc(II) affinity group conjugated to a near-infrared fluorophore. *Bioconjugate Chem.* 2008; 19:686.
18. Johnsen AR, Hausner M, Schnell A, Wuertz S. Evaluation of fluorescently labeled lectins for noninvasive localization of extracellular polymeric substances in *Sphingomonas* biofilms. *Appl. Environ. Microbiol.* 2000; 66:3487. [PubMed: 10919811]
19. Campuzano S, Orozco J, Kagan D, Guix M, Gao W, Sattayasamitsathit S, Claussen JC, Merkoci A, Wang J. Bacterial isolation by lectin-modified microengines. *Nano Lett.* 2012; 12:396. [PubMed: 22136558]
20. Somers WS, Tang J, Shaw GD, Camphausen RT. Insights into the molecular basis of leukocyte tethering and rolling revealed by structures of *P*- and *E*-selectin bound to SLe(X) and PSGL-1. *Cell.* 2000; 103:467. [PubMed: 11081633]
21. Blixt O, Han S, Liao L, Zeng Y, Hoffmann J, Futakawa S, Paulson JC. Sialoside analogue arrays for rapid identification of high affinity siglec ligands. *J. Am. Chem. Soc.* 2008; 130:6680. [PubMed: 18452295]
22. Dam TK, Brewer CF. Thermodynamic studies of lectin-carbohydrate interactions by isothermal titration calorimetry. *Chem. Rev.* 2002; 102:387. [PubMed: 11841248]
23. Komath SS, Kavitha M, Swamy MJ. Beyond carbohydrate binding: New directions in plant lectin research. *Org. Biomol. Chem.* 2006; 4:973. [PubMed: 16525538]
24. Zhou J, Tsai YT, Weng H, Baker DW, Tang L. Real time monitoring of biomaterial-mediated inflammatory responses via macrophage-targeting NIR nanoprobe. *Biomaterials.* 2011; 32:9383. [PubMed: 21893338]



25. Ji T, Muenker MC, Papineni RV, Harder JW, Vizard DL, McLaughlin WE. Increased sensitivity in antigen detection with fluorescent latex nanosphere-IgG antibody conjugates. *Bioconjugate chem.* 2010; 21:427.
26. Jain SK, Jangdey MS. Lectin conjugated gastroretentive multiparticulate delivery system of clarithromycin for the effective treatment of *Helicobacter pylori*. *Mol. Pharmaceutics.* 2009; 6:295.
27. Yin Y, Chen D, Qiao M, Lu Z, Hu H. Preparation and evaluation of lectin-conjugated PLGA nanoparticles for oral delivery of thymopentin. *J. Controlled Release.* 2006; 116:337.
28. Nizet V, Ohtake T, Lauth X, Trowbridge J, Rudisill J, Dorschner RA, Pestonjamas V, Piraino J, Huttner K, Gallo RL. Innate antimicrobial peptide protects the skin from invasive bacterial infection. *Nature.* 2001; 414:454. [PubMed: 11719807]
29. Rey C, Alvarez F, De-La-Rua V, Concha A, Medina A, Diaz JJ, Menendez S, Los-Arcos M, Mayordomo-Colunga J. Intervention to reduce catheter-related bloodstream infections in a pediatric intensive care unit. *Intensive Care Med.* 2011; 37:678. [PubMed: 21271236]
30. Kim JS, Holtom P, Vigen C. Reduction of catheter-related bloodstream infections through the use of a central venous line bundle: Epidemiologic and economic consequences. *Am. J. Infect. Control.* 2011; 39:640. [PubMed: 21641088]
31. Doyle RJ, Birdsall DC. Interaction of concanavalin A with the cell wall of *Bacillus subtilis*. *J. Bacteriol.* 1972; 109:652. [PubMed: 4621684]
32. Ofek I, Mirelman D, Sharon N. Adherence of *Escherichia coli* to human mucosal cells mediated by mannose receptors. *Nature.* 1977; 265:623. [PubMed: 323718]
33. Torrent M, Navarro S, Moussaoui M, Nogues MV, Boix E. Eosinophil cationic protein high-affinity binding to bacteria-wall lipopolysaccharides and peptidoglycans. *Biochemistry.* 2008; 47:3544. [PubMed: 18293932]
34. Xiao J, Zhang H, Niu L, Wang X. Efficient screening of a novel antimicrobial peptide from *Jatropha curcas* by cell membrane affinity chromatography. *J. Agric. Food Chem.* 2011; 59:1145. [PubMed: 21268582]
35. Zhao H, Joseph J, Fales HM, Sokoloski EA, Levine RL, Vasquez-Vivar J, Kalyanaraman B. Detection and characterization of the product of hydroethidine and intracellular superoxide by HPLC and limitations of fluorescence. *Proc. Natl. Acad. Sci. USA.* 2005; 102:5727. [PubMed: 15824309]
36. Zielonka J, Vasquez-Vivar J, Kalyanaraman B. Detection of 2-hydroxyethidium in cellular systems: a unique marker product of superoxide and hydroethidine. *Nat. Protoc.* 2008; 3:8. [PubMed: 18193017]
37. Zhu QS, Chen LB, Zhu PY, Luan JF, Mao C, Huang XH, Shen J. Preparation of PNIPAM-g-P (NIPAM-co-St) microspheres and their blood compatibility. *Colloids Surf., B.* 2013; 10:461.
38. Weng H, Zhou J, Tang L, Hu Z. Tissue responses to thermally-responsive hydrogel nanoparticles. *J. Biomater. Sci. Polym. Ed.* 2004; 15:1167. [PubMed: 15503633]

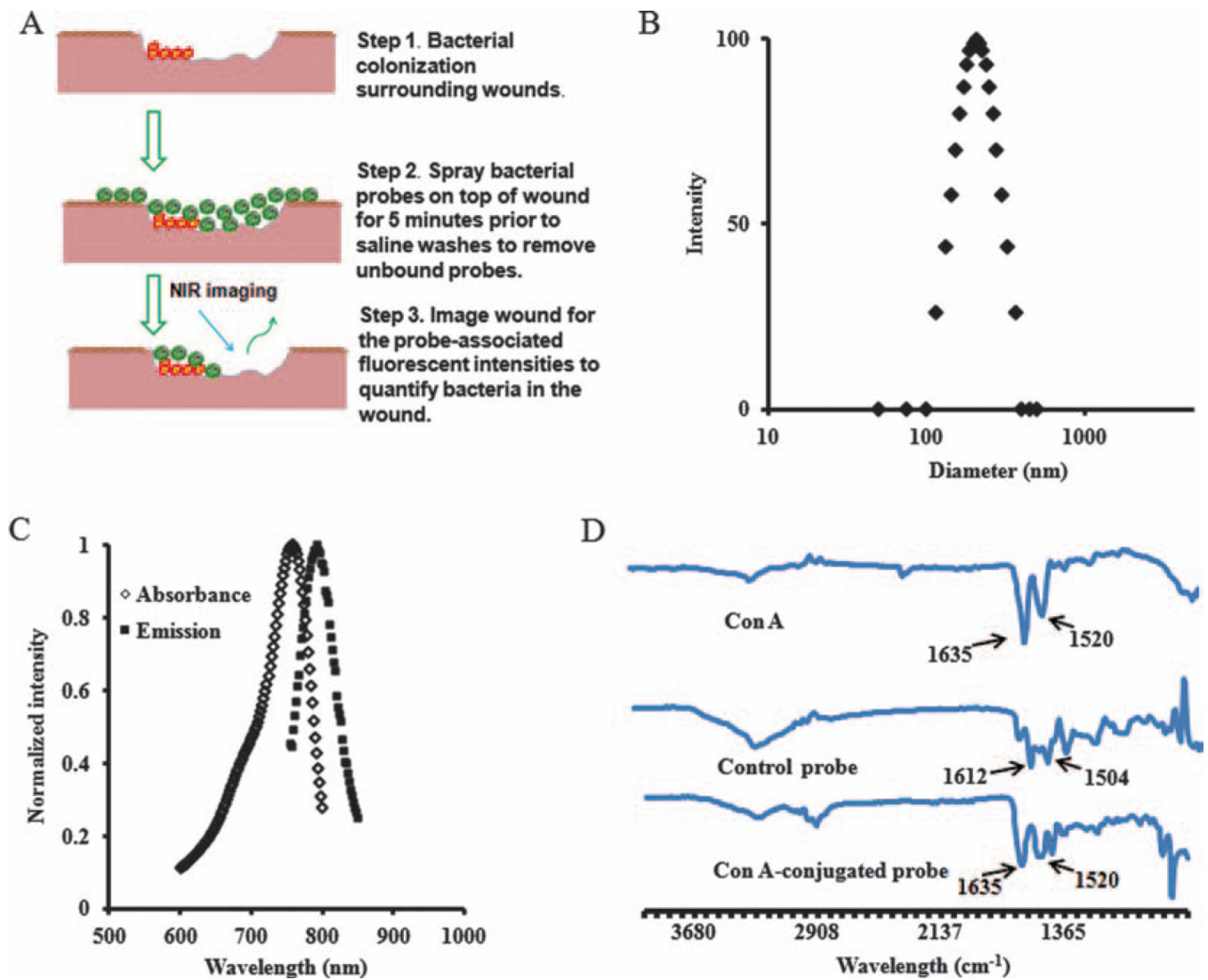


**Figure 1.** (A) Schematic illustration of the bacteria-targeting optical nanoprobe; (B) Nanoprobe size measured by Photon Correlation Spectroscopy; (C) The absorbance and emission of the optical nanoprobe; (D) FTIR spectra of Con A, optical probe and control probe.

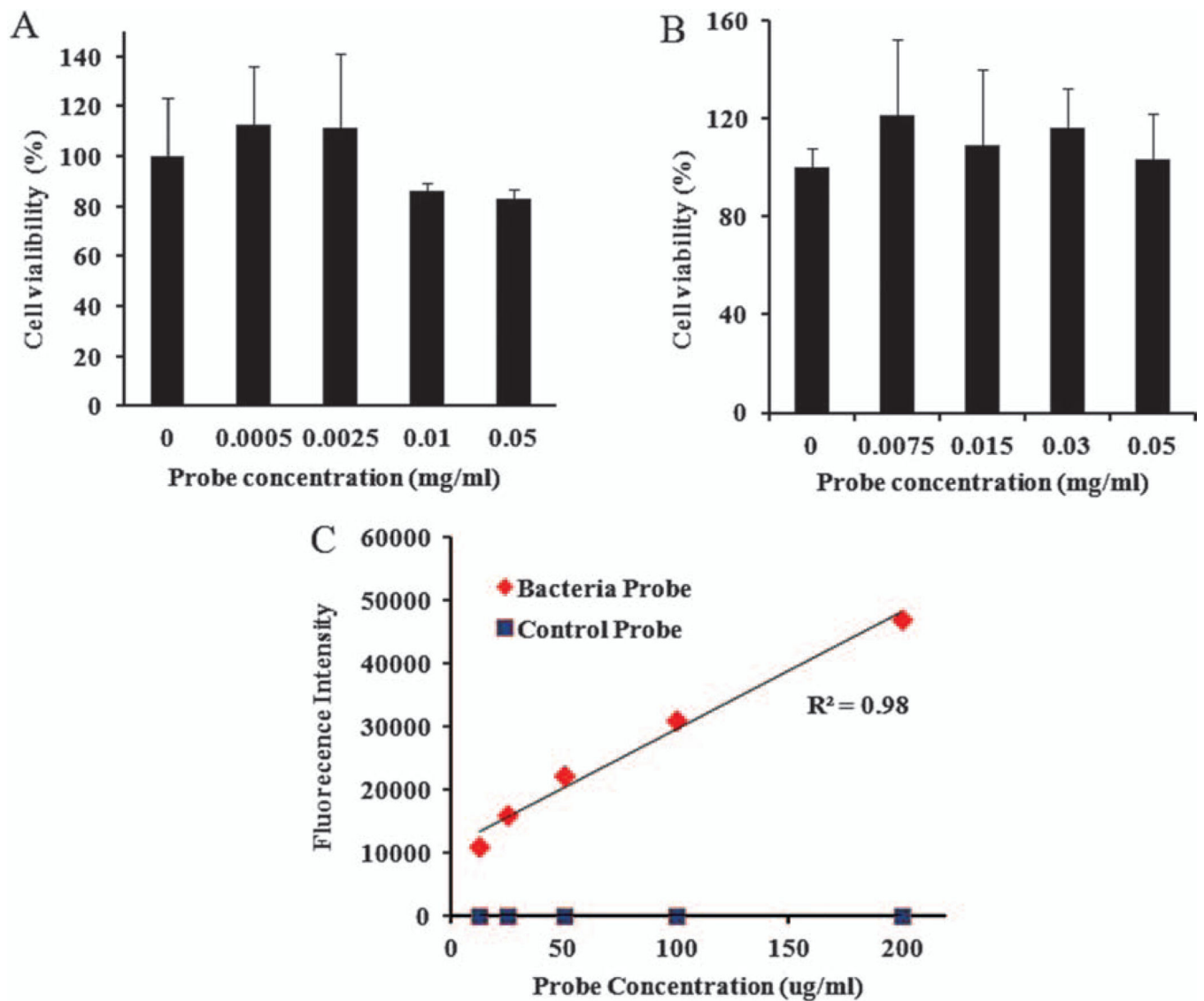


**Figure 2.** Quantitative assessment of bacteria probe cytotoxicity to (A) 3T3 fibroblasts and (B) Raw 264.7 macrophages using MTS assay; (C) *In vitro* investigation of the binding affinity of the bacteria probes and control probes to bacteria. *Staphylococcus aureus* ( $1.6 \times 10^8$  CFU/ml) were incubated with different concentrations of probes (12.5, 25, 50, 100, and 200  $\mu\text{g/ml}$ ) for 30 minutes and followed with 3 $\times$  wash of sterile PBS. The fluorescence intensities of bacteria-bound probes were then determined using a fluorescent plate reader.

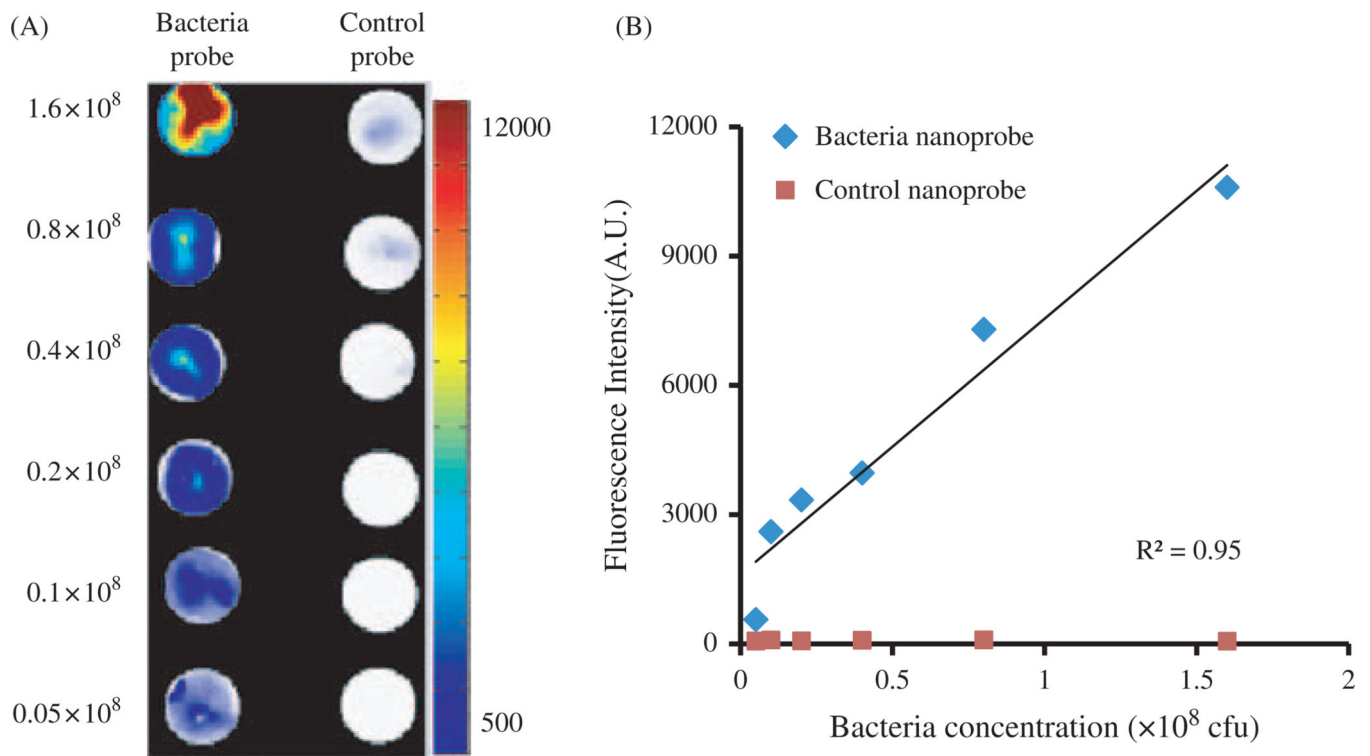


**Figure 3.**

*In vitro* study to assess the specificity of bacteria probes to *Staphylococcus aureus*. (A) Fluorescence microscopy images of bacteria incubated with bacteria probes versus control probes; (B) Correlation between bacteria numbers and bacteria-associated fluorescence intensities following incubation with either bacteria probe or control probe.

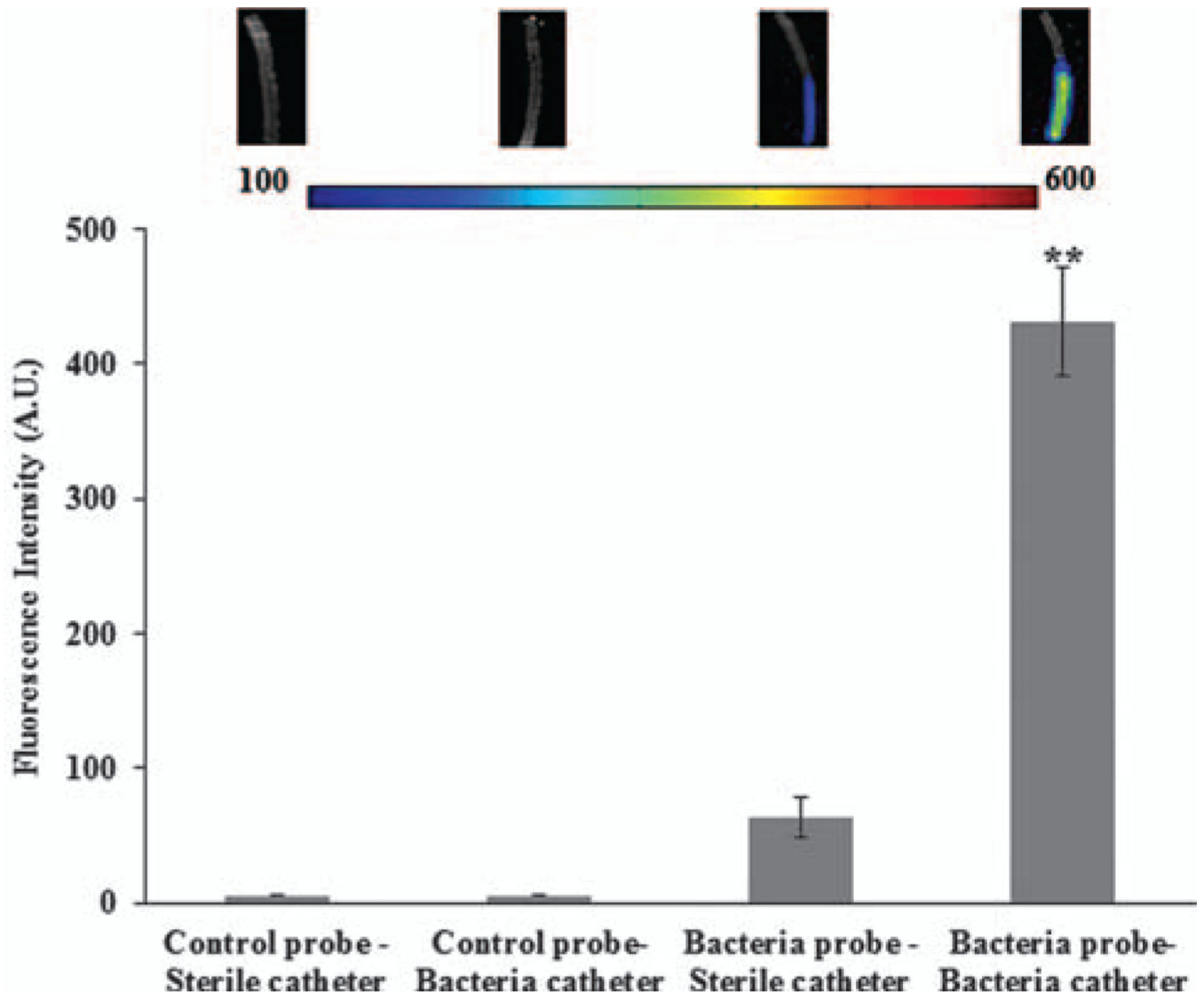


**Figure 4.**

Quantitative analysis of *In vitro* specificity of bacteria probes to *Staphylococcus aureus*. (\*\*, significance vs. control at  $p < 0.01$ ). Infected catheters were prepared by incubation with bacteria solution for 4 hours prior to exposure to either bacteria probe or control probe for 4 minutes. For comparison, sterile catheters were also incubated with either bacteria probe or control probe. (Inserted fluorescence images from left to right: sterile catheter incubated with control probe; bacteria catheter incubated with control probe; sterile catheter incubated with bacteria probe and bacteria catheter incubated with bacteria probe).

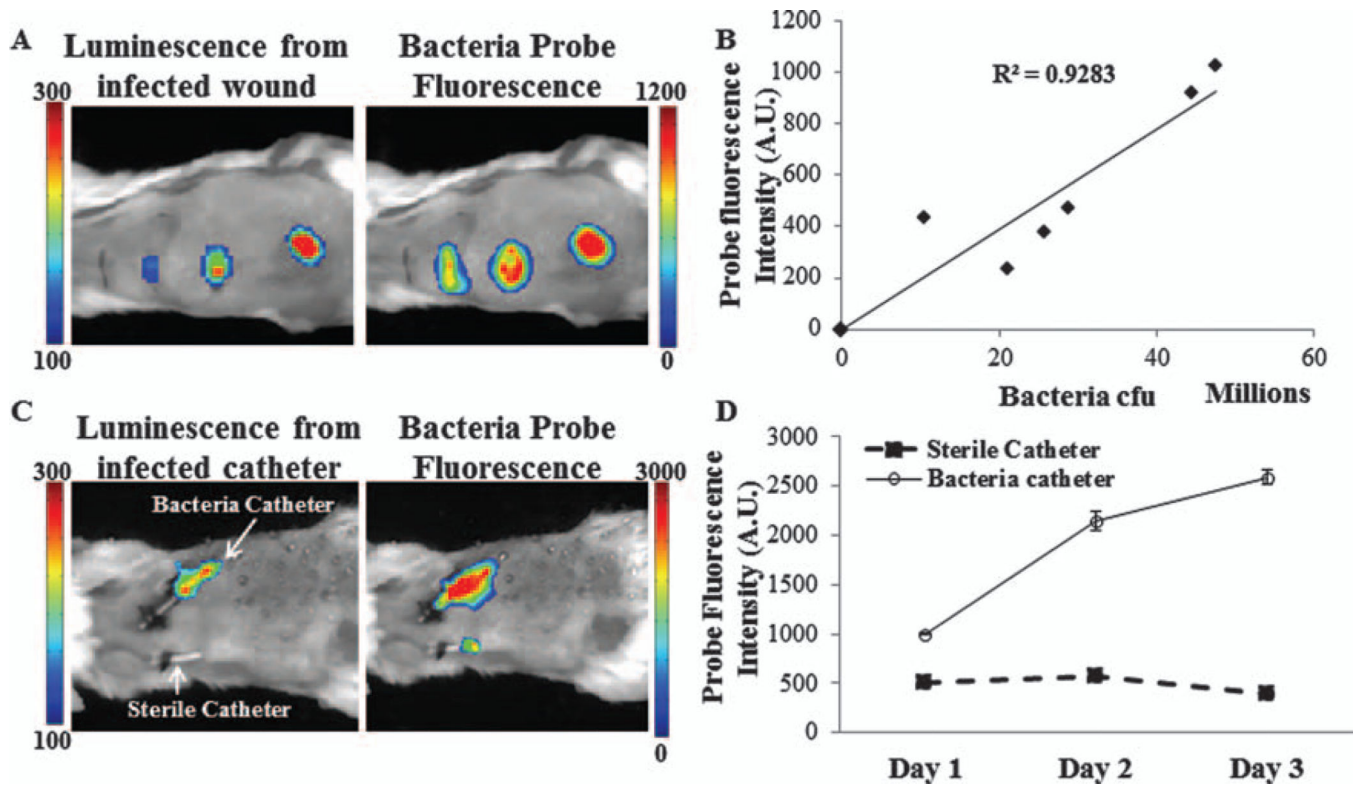


**Figure 5.**

*In vivo* specificity of bacteria probes to *S. aureus*. (A) Increase in fluorescence intensity of the probe and luminescence signal at the infected wound sites. (B) Correlation between probe fluorescence intensities and bacteria numbers. (C) Enhanced fluorescent intensities at the site of infected catheters in comparison with control sterile catheters. (D) Quantitative data comparing the increase in fluorescence of the probe at the infected catheter site versus controls from day 1 to 3.